ROS induces epithelial-mesenchymal transition via the TGF-β1/PI3K/Akt/mTOR pathway in diabetic nephropathy

QIAN LU[1*], WEN-WEN WANG[2*], MING-ZHU ZHANG[3], ZHONG-XUAN MA[1], XIN-RAN QIU[1], MENGLI SHEN[1] and XIAO-XING YIN[1]

[1]Department of Pharmacy, Jiangsu Key Laboratory of New Drug Research and Clinical Pharmacy, Xuzhou Medical University, Xuzhou, Jiangsu 221004; [2]Department of Pharmacy, Wuxi Higher Health Vocational Technology School, Wuxi, Jiangsu 214000; [3]Deparment of Clinical Pharmacy, Changzhou Fourth People's Hospital, Changzhou, Jiangsu 213000, P.R. China

Received August 4, 2017; Accepted March 9, 2018

DOI: 10.3892/etm.2018.7014

Abstract. Oxidative stress has been reported to serve an important role in the development and progression of diabetic nephropathy (DN). Epithelial-mesenchymal transition (EMT) of renal tubular epithelial cells promotes renal fibrosis in DN, while the mechanism of reactive oxygen species (ROS)-mediated EMT is not fully understood. The aim of the present study was to investigate the effect of high glucose-induced ROS on the activation of the transforming growth factor (TGF)-β1/phosphoinositide 3 kinase (PI3K)/protein kinase B (Akt)/mammalian target of rapamycin (mTOR) pathway in a normal rat kidney tubular epithelial cell line (NRK-52E) and rats with type 1 diabetes. *In vitro*, high glucose-stimulated ROS production resulted in increased TGF-β1 expression as well as an increase in the Akt and mTOR phosphorylation ratio, resulting in EMT. When cells were pre-treated with ROS inhibitors, changes in TGF-β1, Akt and mTOR were significantly ameliorated. *In vivo*, diabetic rats experienced a significant decline in renal function and severe renal fibrosis compared with control rats at 8 weeks following streptozocin injection. Levels of malondialdehyde and TGF-β1/PI3K/Akt/mTOR pathway activation were increased in the renal cortex of rats with diabetes compared with the control rats. Furthermore, renal fibrosis was further aggravated in DN compared with the control rats. The results of the present study suggest that ROS serves an important role in mediating high glucose-induced EMT and inhibits activation of the TGF-β1/PI3K/Akt/mTOR pathway. ROS may therefore have potential as a treatment approach to prevent renal fibrosis in DN.

Correspondence to: Professor Xiao-Xing Yin, Department of Pharmacy, Jiangsu Key Laboratory of New Drug Research and Clinical Pharmacy, Xuzhou Medical University, 209 Tongshan Road, Xuzhou, Jiangsu 221004, P.R. China
E-mail: yinxx@xzhmu.edu.cn

*Contributed equally

Key words: diabetes, reactive oxygen species, epithelial-mesenchymal transition, transforming growth factor-β1, phosphoinositide 3 kinase, protein kinase B, mammalian target of rapamycin

Introduction

Diabetic nephropathy (DN) is a major chronic complication of diabetes and leads to end-stage renal disease (1). DN is characterized by glomerular hypertrophy, thickening of the basement membrane and glomerulosclerosis during the early stage, while tubular atrophy or interstitial fibrosis occur during the late stage, ultimately leading to a loss of renal function (1,2). Interstitial fibrosis is an inevitable result of chronic kidney disease (CKD) (3). Epithelial-mesenchymal transition (EMT) has been implicated as a major pathway leading to the generation of renal interstitial fibrosis in DN (4-7). During EMT, epithelial cells lose several epithelial characteristics, such as epithelial (E)-cadherin, and acquire properties typical of mesenchymal cells such as α-smooth muscle actin (α-SMA) (8). However, the molecular mechanisms underlying the development of renal interstitial fibrosis have not been fully elucidated.

It is known that reactive oxygen species (ROS) serve an important role in the development of diabetic complications (9). ROS overproduction in the diabetic microenvironment occurs as a direct consequence of hyperglycaemia (10). ROS includes molecular oxygen and its derivatives (11) and are known to function as second messengers. It has been reported that high glucose (HG)-induced ROS overexpression is the unifying mechanism of diabetic complications (11,12). As such, inhibiting ROS production may be beneficial for the treatment of DN.

Transforming growth factor-β1 (TGF-β1) is a potent inducer of EMT and there is evidence of TGF-β1-induced EMT in tubular epithelial cells and kidney tissues (13,14). A number of studies have investigated the associated signalling pathways, including mitogen-activated protein kinase (MAPK) (15), Smad proteins (16) and phosphatidylinositol 3-kinase (PI3K)/protein kinase B (Akt) (17). Akt is a subfamily of serine/threonine kinases and serves a role in a number of

signalling circuits (18). Previous studies by our group have revealed that Akt phosphorylation is increased in rat mesangial cells under HG conditions, as well as in kidney tissues from db/db mice (19,20). Mammalian target of rapamycin (mTOR), a downstream protein of PI3K/Akt, is a new member of the phosphatidylinositol kinase associated kinase (PIKK) family and serves an important role in cell proliferation, differentiation, metastasis and survival (21). mTOR kinase as two different polyprotein complexes, mTORC1 and mTORC2, whose subunit composition consists of upstream inputs and downstream substrates, which function differently (22). Despite the presence of mTOR in both complexes, only mTORC1 is sensitive to rapamycin inhibition (23). It has previously been reported that the mTOR signalling pathway serves a role in the onset and progression of DN, while mTOR inhibition by rapamycin is able to prevent DN progression in animals with type 1 and type 2 diabetes mellitus (23).

It is well known that ROS regulates Akt/mTOR signalling (24,25) and mTOR serves a role in DN and TGF-β1 induced EMT (26-28); however, the association between HG-induced ROS production and the TGF-β1/PI3K/Akt/mTOR pathway has not been fully elucidated. It is therefore necessary to further explore whether the activation of PI3K/Akt/mTOR signalling induced by ROS under high-glucose conditions affects EMT in DN.

Materials and methods

Cell culture. Normal rat kidney tubular epithelial cell line (NRK-52E) cells were donated by Mrs Chen Sha from the Nanjing University of Traditional Chinese Medicine (Nanjing, China). Cells were cultured in Dulbecco's modified Eagle's medium (DMEM; Gibco; Thermo Fisher Scientific, Inc., Waltham, MA, USA) at 37˚C in a humidified atmosphere containing 5% CO_2 and 95% air. The cells passaged three times per week. Prior to use, cells were synchronized for 24 h, followed by treatment with 54.4 mmol/l mannitol (MA), 20 μmol/l dimethlysulfoxide (DMSO), 60 mmol/l glucose (also known as HG), 1x10^{-5} mol/l H_2O_2, 10 ng/ml TGF-β1, HG + 50 μmol/l antioxidant N-acetylcysteine (NAC), HG + 10 μmol/l inhibitor of TGF-β1 (SB-431542), HG + 20 μmol/l inhibitor of PI3K (LY-294002) or HG + 20 nmol/l inhibitor of mTOR (rapamycin; Cell Signalling Technology, Inc., Danvers, MA, USA). Cells were treated as indicated for 48 h, the cells were assessed using an inverted light microscope (magnification, x200) and then harvested for analysis. NAC, SB-431542 and LY-294002 were provided by Sigma-Aldrich (Merck KGaA, Darmstadt, Germany). The normal glucose (NG), NG+MA, HG and HG+DMSO groups were assessed and micrographs were captured at 48 h using an inverted light microscope (magnification, x400). MA was used as an agent to simulate the osmotic pressure of a high-glucose condition and DMSO was used as a solvent.

Animals and study protocol. A total of 20 male Wistar rats at the age of 8 weeks, weighing 200-220 g, were housed in the Experimental Animal Center of Xuzhou Medical University (Xuzhou, China). Rats were provided with free access to food and water. The animal room was maintained at 24±1˚C, with relative humidity between 40 and 60% and a 12-h light/dark cycle. A total of 10 rats were administered with 60 mg/kg streptozocin (STZ; Sigma Aldrich; Merck KGaA) dissolved in 0.01 mol/l citrate buffer (pH 4.5; Beyotime Institute of Biotechnology) via intraperitoneal injection to induce diabetes mellitus. At 3 days after STZ administration, fasting blood glucose levels were measured using blood glucose test strips and the OneTouch UltraEasy glucose meter (both LifeScan, Inc.; Johnson & Johnson Services, Inc., New Brunswick, NJ, USA) and a value of >13.9 mmol/l was considered to indicate diabetes. The rats that did not receive treatment were placed in the normal control (N) group, those with fasting blood glucose levels >13.9 mmol/l were place in the diabetes mellitus (DM) group (10 rats/group). After 8 weeks, rats were placed in metabolic cages (DXL-D; Beijing Jiayuan Industrial Technology Co., Ltd., Beijing, China) for 24 h of urine collection. Then the rats were sacrificed, blood was collected from the abdominal aorta and the serum was separated from the cells by centrifugation of the blood at 3,000 x g for 15 min at 20˚C. Kidneys were also removed and the kidney cortexes were isolated. The samples were stored at -80˚C for biochemical analysis. The present study was approved by the Animal Ethics Committee of Xuzhou Medical University (Xuzhou, China) and all experiments were performed in accordance with the Guidelines for Ethical Conduct in the Care and Use of Animals.

Renal function assessment and antioxidant index. Indicators of renal function were assessed, including 24-h urine protein, serum creatinine (Cr) and blood urea nitrogen (BUN). The levels of GSH and T-SOD were measures to determine the antioxidant index in the renal cortex and serum in diabetic rats. Cr and BUN assay kits were purchased from Changchun Huili Biotech Co., Ltd. (Changchun, China). Levels of urine protein, glutathione (GSH; cat. no. A006-2) and superoxide dismutase (T-SOD; cat. no. A001-3) were measured using kits (Nanjing Jiancheng Bioengineering Institute, Nanjing, China).

Periodic acid-Schiff (PAS) staining. Kidney tissues were fixed in 4% formaldehyde for 48 h at room temperature and embedded in paraffin for histological analysis. Then, the 3-μm-thick sections were dewaxed and hydrated. The sections were stained with PAS (cat. no. DG0005; Beijing Leagene Biotech. Co., Ltd., Beijing, China) for 15 min at room temperature, dehydrated to transparency and mounted with neutral gum. The sections were examined using a light microscope (BX43F; Olympus Corporation, Tokyo, Japan; magnification, x400). The three most central sections were analysed. Linear measurements were obtained with an image analysis system (Image-Pro Plus 4.0; Media Cybernetics, Inc., Rockville, MD, USA).

Masson staining. Kidneys sections (3-μm-thick) were stained with a Masson assay kit (cat. no. 16071; Shanghai Yuanye Biotechnology Co., Ltd., Shanghai, China) according to the manufacturer's protocol. The sections were examined using a light microscope (magnification, x400), and the green zones, which mainly consisted of collagen, were measured by Image-Pro Plus 4.0 software.

High performance liquid chromatography (HPLC). Malondialdehyde (MDA), an indicator of oxidative stress injury, was measured using HPLC. Kidneys were dissected

Table I. Primer sequences and product lengths.

Gene	Direction	Sequence (5'-3')	Length (bp)
Transforming growth factor-β1	F	TGCTTCAGCTCCACAGAGAA	182
	R	TGGTTGTAGAGGGCAAGGAC	
Endothelial cadherin	F	CACACTGATGGTGAGGGTACAAGG	123
	R	GGGCTTCAGGAACACATACATGG	
α-smooth muscle actin	F	CGGGCTTTGCTGGTGATG	143
	R	GGTCAGGATCCCTCTCTTGCT	
β-actin	F	CCCATCTATGAGGGTTACGC	150
	R	TTTAATGTCACGCACGATTTC	

F, forward; R, reverse

and homogenized in pre-chilled 0.9% neutral normal saline. The resultant homogenate was centrifuged at 4˚C at 2,500 x g for 10 min and the supernatant was kept for further analysis. For alkaline hydrolysis of protein bound MDA, 20 μl 6 mol/l sodium hydroxide was added to 100 μl supernatant, and the sample was incubated in a 60˚C water bath for 30 min, and then incubated in ice. The hydrolyzed sample was acidified with 50 μl 35% perchloric acid. The resulting suspension was then vortexed for 30 sec and centrifuged at 12,000 x g for 10 min at 4˚C. The less dense, clear supernatant (150 μl) was mixed with 15 μl of Brady's reagent (5 mmol/l Brady's reagent and 2 mol/l HCl) and incubated for 30 min at room temperature for derivatization. Following derivatization, the samples were filtered through a 0.2 μm filter.

Aliquots of 50 μl were injected into a HPLC system. MDA levels were measured by reversed-phase (RP)-HPLC with pre-column derivatization on an Agilent Zorbax SB-C18 column (4.6x150 mm, 5 μm; Agilent Technologies, Inc., Santa Clara, CA, USA). The mobile phase consisted of acetonitrile-distilled water (38:62, v/v) containing 0.2% acetic acid at a flow rate of 1 ml/min. The RP column was set at room temperature and a wavelength of 310 nm was used for UV detection. The concentration of MDA was calculated based on a standard curve and expressed as nmol/g protein. The MDA standard was prepared by dissolving 1,1,3,3-tetraethoxypropane (TEP) in water to give a stock solution of 1 mmol/l. The working standard was prepared by serial dilution of the TEP stock solution with 1% sulfuric acid to 20, 10, 5, 2.5, 1.25, 0.625, 0.3125 and 0.15625 μmol/l, yielding a standard curve for total MDA content determination.

Flow cytometry. To evaluate the intracellular generation of ROS, cells were cultured for 48 h at 37˚C with the indicated treatments. Cells were seeded (10,000 cells) in 6-well plates and incubated in serum-free DMEM for 24 h. Cells were then washed with serum-free DMEM and then incubated with 2', 7'-dichlorofluorescein diacetate (DCFH-DA; Beijing Bioleb Technology Co., Ltd., Beijing, China) at 37˚C for 20 min. Changes in intracellular ROS levels were then determined by measuring the oxidative conversion of cell permeable DCFH-DA to fluorescent dichlorofluorescein (DCF) using a ROS detection kit (Beyotime Institute of Biotechnology, Haimen, China). The DCF fluorescence distribution of the cells was detected at excitation and emission wavelengths of 488 and 525 nm, respectively, by a MACSQuant VYB flow cytometer (Miltenyi Biotec GmbH, Bergisch Gladbach, Germany) and quantified by the internal software.

ELISA. NRK-52E cells were seeded into a 12-well plate at a density of $1.0x10^6$ cells/well. The cells were then incubated in serum-free DMEM for 24 h, the medium was discarded and 2 ml of the treatment was added: 54.4 mmol/l MA, 20 μmol/l DMSO, 60 mmol/l glucose, $1x10^{-5}$ mol/l H_2O_2, 10 ng/ml TGF-β1, HG + 50 μmol/l NAC, HG + 10 μmol/l SB-431542, HG + 20 μmol/l LY-294002 or HG + 20 nmol/l rapamycin. After 48 h of continuous culturing, the culture supernatant was collected and the concentration of TGF-β1 was measured according to a TGF-β1 ELISA kit (cat. no. T10201-09; Shanghai Boyun Biotech Co., Ltd., Shanghai, China).

RNA isolation and reverse transcription-quantitative polymerase chain reaction (RT-qPCR). cDNA was isolated from NRK-52E cells and kidney cortices using the TRIzol reagent (Invitrogen; Thermo Fisher Scientific, Inc.) according to the manufacturer's protocol. An RT-Rever TraAce qPCR RT kit (Toyobo Life Science, Osaka, Japan), gene-specific primers and SYBR-Green I Master Mix (Roche Diagnostics, Basel, Switzerland) were used for PCR. Primers were purchased from Sangon Biotech Co., Ltd. (Shanghai, China) and are presented in Table I. The PCR reactions were performed in a Light Cycle 480 System (Roche Applied Science, Mannheim, Germany) as previously described (29), using a thermal profile of 10 min at 95˚C, followed by 40 cycles of 15 sec at 95˚C, 30 sec at 60˚C, then a melting curve of 15 sec at 95˚C, 60 sec at 1 min. The samples were heating to 95˚C and cooled for 30 sec at 4˚C. The results were quantified using the $2^{-\Delta\Delta Cq}$ method (30).

Western blotting. Cultured NRK-52E cells were harvested in lysis buffer containing 50 mmol/l Tris (pH 7.6), 150 mmol/l NaCl, 1 mmol/l EDTA, 1% NP-40, 1 mmol/l PMSF, 1 mmol/l Na_3VO_4 and 20 mmol/l NaF on ice. Homogenates from the renal cortexes were prepared using RIPA lysis buffer containing 50 mmol/l Tris (pH 7.4), 150 mmol/l NaCl, 1% TritonX-100, 1% sodium deoxycholate, 0.1% SDS, 1 mmol/l

PMSF, 1 mmol/l Na_3VO_4 and 20 mmol/l NaF on ice. The supernatant was collected after centrifugation at 12,000 x g at 4˚C for 15 min. Protein concentrations were determined using a bicinchoninic acid protein assay (Thermo Fisher Scientific, Inc.) according to the manufacturer's protocol. Equal amounts of protein (40 μg of the *in vitro* proteins and 80 μg/lane of the *in vivo* proteins) were separated by 8% SDS-PAGE and transferred onto nitrocellulose membranes. The membranes were blocked in tris-buffered saline with Tween-20 containing 3% bovine serum albumin (Sigma Aldrich; Merck KGaA) for 1 h at room temperature. Membranes were subsequently incubated with antibodies against the following: Akt, phosphorylated-Akt (Ser473; 1:1,000; cat. no. BS1810), E-cadherin (1:1,000; cat. no. BS1347) and β-actin (1:1,000; cat. no. AP0060; all Bioworld Technology, Inc., St. Louis Park, MN, USA), mTOR (1:1,000; cat. no. 2983) and phosphorylated-mTOR (Ser2448; 1:1,000; cat. no. 5536; Cell Signalling Technology, Inc.) and α-SMA (1:1,000; cat. no. M0851; Dako; Agilent Technologies, Inc., Santa Clara, CA, USA) overnight at 4˚C. The primary antibodies were detected using alkaline phosphatase-conjugated immunoglobulin G antibodies (cat. no. SA00002-2; Bioworld Technology, Inc.) for 1 h at room temperature. An immunoblot was generated using the ECL western blotting detection system (Thermo Fisher Scientific, Inc.). Bands were quantified using ImageJ software (version 1.3.4.67; National Institutes of Health, Bethesda, MD, USA).

Wound healing assay. Cell migration behaviour was assessed using a wound healing assay. Cells were seeded in 6-well plates ($1x10^5$ cells/well) and grown to 80% confluence at 37˚C. The cell monolayer was scratched with a pipette tip (Axygen; Corning Incorporated, Corning, NY, USA) to create a narrow wound-like gap. Shortly after wounding, the NRK-52E cells were washed with PBS twice and incubated with the indicated treatments at room temperature. Plates were assessed and micrographs were captured at 0, 12 and 24 h using an inverted light microscope (magnification, x400). The number of migrated cells was quantified by manual counting and six randomly chosen fields were analysed for each well.

Cell invasion assays. An invasion assay was performed to evaluate the effect of HG and ROS on the invasion ability of NRK-52E cells. Transwell chambers were initially coated with Matrigel (40 μg/100 μl/chamber) at 37˚C for 1 h. The cells were suspended in DMEM ($5x10^5$ cells/ml) and seeded in the upper compartment, while DMEM containing 10% fetal bovine serum (Gibco; Thermo Fisher Scientific, Inc.) was added in the lower compartment. Chambers were incubated in an atmosphere containing 5% CO_2 at 37˚C for 24 h and non-invaded cells on the upper side of the membrane were removed with a cotton swab. The invaded cells on the bottom surface were fixed with 100% methanol for 30 min and stained with haematoxylin and eosin (Nanjing Sunshine Biotechnology Co., Ltd., Nanjing, China) for 15 min at room temperature. Invaded cells were quantified by manual counting using an inverted light microscope (magnification, x400) and five randomly chosen fields were analysed for each group.

Statistical analysis. All data are presented as the mean ± standard error of the mean. Statistical analysis was performed using SPSS version 13 (SPSS, Inc., Chicago, IL, USA). Comparisons between groups were made using one-way analysis of variance followed by the Student-Newman-Keuls test. $P<0.05$ was considered to indicate a statistically significant difference.

Results

The effects of osmotic pressure and solvent. The effects of MA and DMSO on the indices investigated in our study were assessed, including morphologic changes of NRK-52E cells, intracellular ROS production, E-cadherin expression and α-SMA expression. The levels of these indices in the MA group were almost identical to those in the normal standard group, indicating that the osmotic pressure generated by HG did not affect any of the indices involved (Fig. 1). All indices in the DMSO group were similar compared with the HG+DMSO group, indicating that DMSO had no significant effects on the results (Fig. 1). Based on these data, the NRK-52E cells in the NG group were incubated in DMEM with 5.56 mmol/l of glucose and 54.44 mmol/l of MA, while NRK-52E cells in the HG+DMSO group were incubated in DMEM with 60 mmol/l of glucose and 20 μmol/l of DMSO for subsequent experiments.

HG induces oxidative stress in NRK-52E cells. Intracellular ROS generation in NRK-52E cells was assessed. Sustained HG or H_2O_2 stimulation for 48 h significantly increased ROS generation compared with the NG+MA group (Fig. 2A). In cells incubated with the antioxidant NAC, LY-294002 or rapamycin, intracellular ROS production was significantly decreased compared with the NG+MA group (Fig. 2A). These results suggest that HG stimulation is able to induce ROS production in NRK-52E cells and that the antioxidant NAC is able to effectively inhibit the increased ROS generation in HG conditions.

HG promotes the expression of TGF-β1 via the overproduction of ROS in NRK-52E cells. H_2O_2 was used to simulate oxidative stress. The expression of TGF-β1 protein was measured using ELISA and the relative quantity of TGF-β1 was assessed using RT-qPCR. The results revealed that, compared with the NG+MA group, the TGF-β1 protein (Fig. 2B) and mRNA (Fig. 2C) expression was significantly increased in the HG+DMSO group and H_2O_2 groups. In the NAC group, the levels of TGF-β1 mRNA and protein were significantly decreased compared with the HG+DMSO group (Fig. 2B and C); however, treatment with the PI3K inhibitor LY-294002 had no significant effect (Fig. 2B and C). Taken together, these results suggest that ROS overproduction stimulates the expression of TGF-β1 in HG conditions.

HG promotes PI3K/Akt/mTOR signalling via ROS and TGF-β1 in NRK-52E cells. To evaluate the effect of ROS and TGF-β1 on PI3K/Akt/mTOR signalling in NRK-52E cells, the phosphorylation levels of Akt (Ser473) and mTOR (Ser2448) in HG conditions were detected by western blotting. The expression of phosphorylated Akt and mTOR were significantly increased in the HG+DMSO, H_2O_2 and TGF-β1 groups compared with the NG+MA group (Fig. 2D and E). In contrast, treatment with SB-431542 (TGF-β1 inhibitor), LY-294002 or NAC

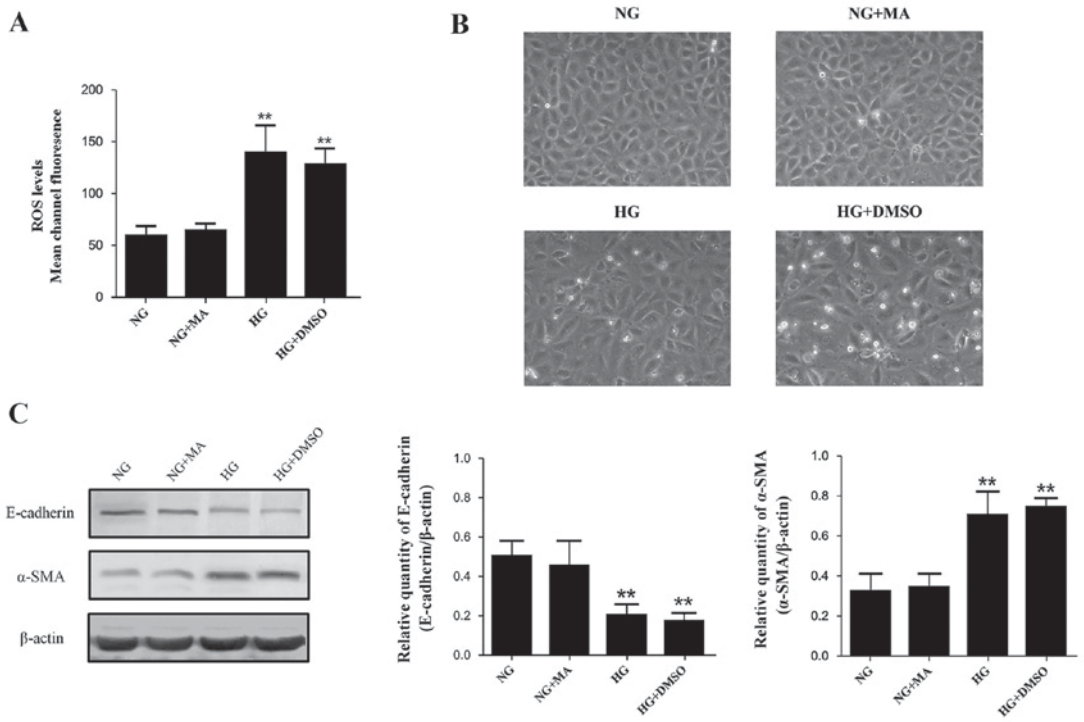

Figure 1. Effects of osmotic pressure and different solvents on ROS production and EMT in NRK-52E cells. Effects of MA and DMSO on (A) intracellular ROS production, (B) morphological changes and (C) the expression of E-cadherin and α-SMA. ROS, reactive oxygen species; EMT epithelial-mesenchymal transition; MA, mannitol; DMSO, dimethylsulfoxide; E-cadherin, epithelial cadherin; SMA, smooth muscle actin; NG, normal glucose (5.56 mmol/l); HG, high glucose (60 mmol/l). **P<0.01 vs. NG.

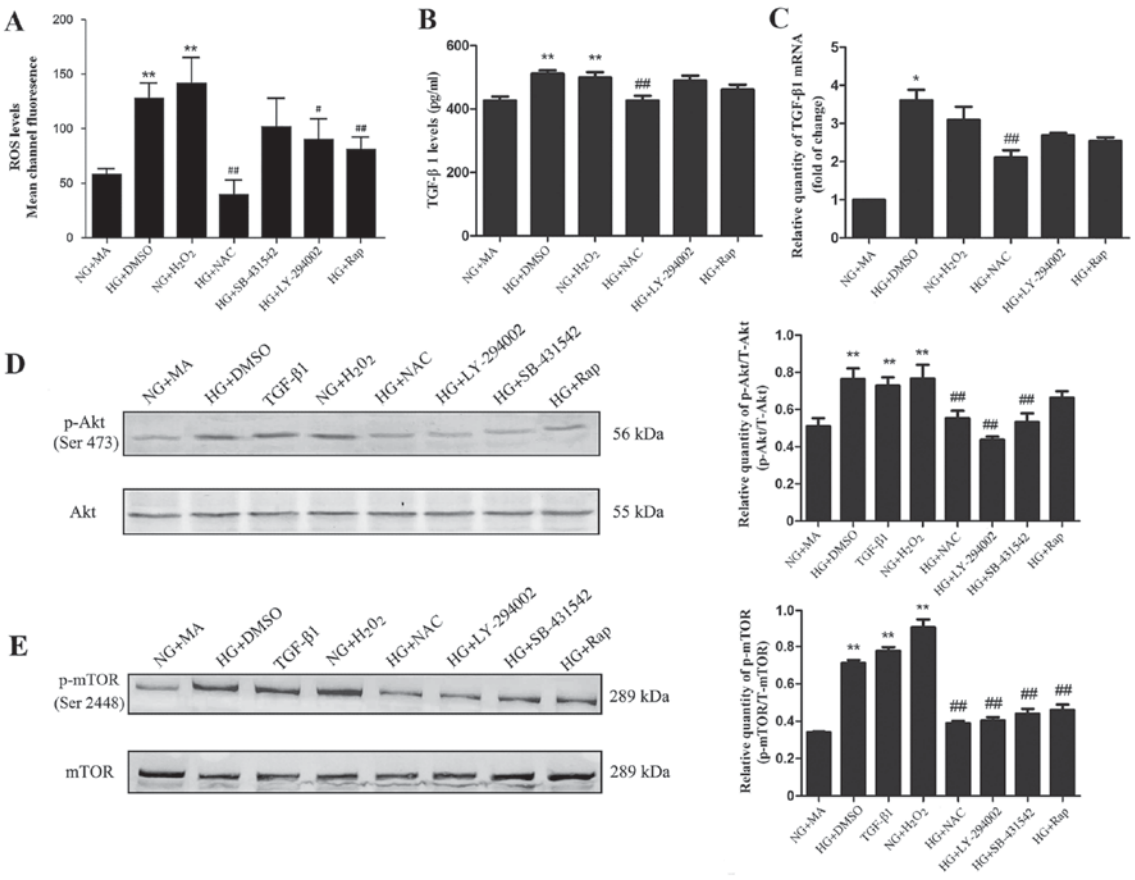

Figure 2. Effect of HG on (A) ROS, (B) TGF-β1 protein, (C) TGF-β1 mRNA, (D) p-Akt and (E) p-mTOR in NRK-52E cells. Cells were starved for 24 h and treated as indicated for 48 h. *P<0.05 and **P<0.01 vs. NG+MA; $^{\#}$P<0.05 and $^{\#\#}$P<0.01 vs. HG. HG, high glucose (60 mmol/l); ROS, reactive oxygen species; TGF, transforming growth factor; p, phosphorylated; Akt, protein kinase B; mTOR, mammalian target of rapamycin; NG, normal glucose (5.56 mmol/l); MA, mannitol; DMSO, dimethylsulfoxide; NAC, N-acetylcysteine; Rap, rapamycin.

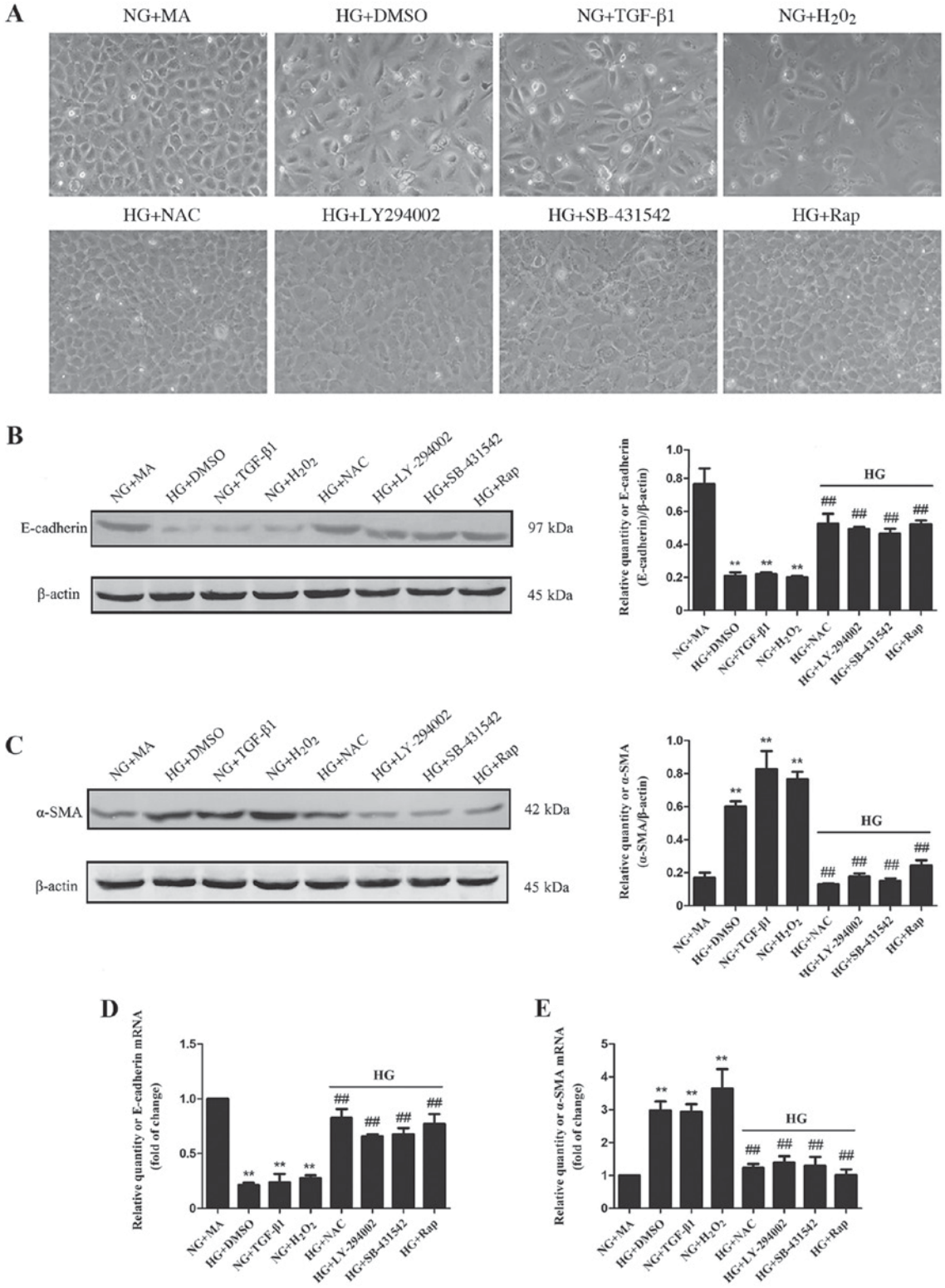

Figure 3. Effects of HG and different factors on EMT in NRK-52E cells. (A) Morphological changes, (B) E-cadherin protein expression, (C) α-SMA protein expression, (D) E-cadherin mRNA expression and (E) α-SMA mRNA expression in NRK-52E cells. **P<0.01 vs. NG+MA and $^{\#\#}$P<0.01 vs. HG. HG, high glucose (60 mmol/l); EMT, epithelial-mesenchymal transition; E-cadherin, epithelial cadherin; SMA, smooth muscle actin; NG, normal glucose (5.56 mmol/l); MA, mannitol; DMSO, dimethylsulfoxide; TGF, transforming growth factor; NAC, N-acetylcysteine; Rap, rapamycin.

resulted in a significant decrease in phosphorylated Akt and mTOR compared with the NG+MA group (Fig. 2D and E). Treatment with rapamycin significantly decreased the phosphorylation of mTOR and had no significant effect on the phosphorylation of Akt (Fig. 2D and E). These results suggest that PI3K/Akt/mTOR signalling may be induced by ROS and TGF-β1.

HG induces the EMT via an ROS-mediated mechanism in NRK-52E cells. EMT of tubular epithelial cells is the

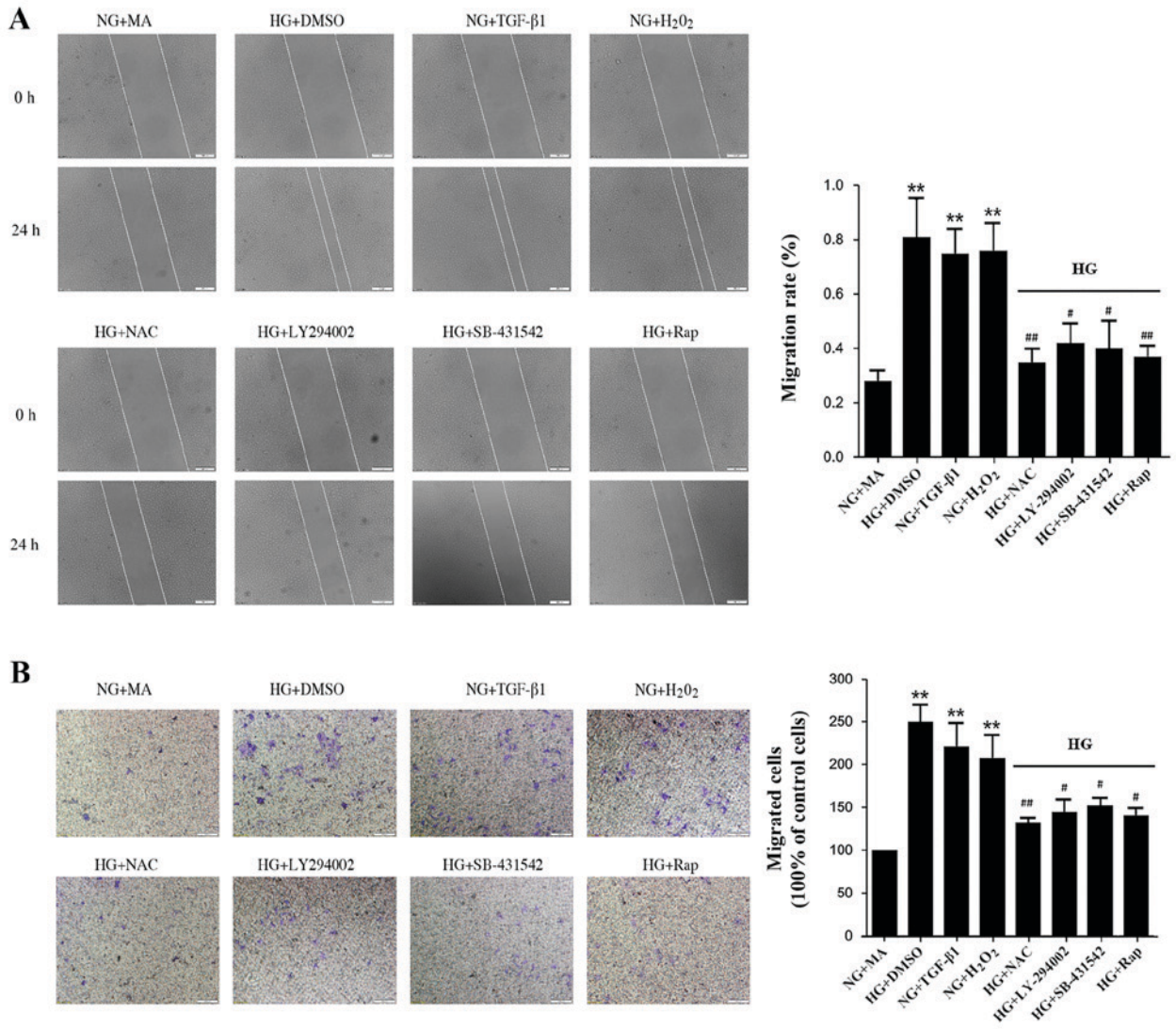

Figure 4. Effects of HG and different factors on cell migration and invasion. (A) The cell monolayer was wounded using a 200 ml yellow pipette tip followed by treatment with different factors for 24 h. The number of the cells in the denuded zone was quantified under an inverted microscope. White lines indicate the wound edge. Magnification, x100. (B) Invading cells were stained with hematoxylin and eosin and quantified. Magnification, x200. **P<0.01 vs. NG+MA; $^{\#}$P<0.05 and $^{\#\#}$P<0.01 vs. HG+DMSO. HG, high glucose (60 mmol/l); NG, normal glucose (5.56 mmol/l); MA, mannitol; DMSO, dimethylsulfoxide; TGF, transforming growth factor; NAC, N-acetylcysteine; Rap, rapamycin.

leading cause of kidney fibrosis (5). To investigate whether EMT is induced by ROS, TGF-β1 and the PI3K/Akt/mTOR signalling pathway, morphological changes of NRK-52E cells were assessed under a microscope. Cells in the HG+DMSO, TGF-β1 and H_2O_2 groups lost their pebbled epithelial appearance and obtained a spindle-shaped fibrous shape compared with cells in the NG+MA group (Fig. 3A). Furthermore, compared with the HG+DMSO group, treatment with antioxidant NAC, SB-431542, LY-294002 and rapamycin markedly inhibited these morphological changes (Fig. 3A). To further evaluate the roles of different factors in renal fibrosis, the epithelial EMT marker E-cadherin and mesenchymal-type marker α-SMA were assessed using western blotting and RT-qPCR. Compared with the NG+MA group, E-cadherin was significantly decreased in the HG+DMSO, TGF-β1 and H_2O_2 groups, while α-SMA was significantly increased (Fig. 3B-E). Furthermore, treatment with NAC, LY-294002, SB-431542 or rapamycin significantly increased E-cadherin expression and decreased α-SMA expression compared with the HG+DMSO group (Fig. 3B-E). These results suggest that EMT may occur due to the ROS-induced activation of TGF-β1/PI3K/Akt/mTOR signalling under HG conditions.

HG induces migration and invasion via an ROS-mediated mechanism in NRK-52E cells. EMT is associated with enhanced cellular motility, and so cell migration was assessed in the present study. The wound closure rate of NRK-52E cells increased significantly in the HG+DMSO, H_2O_2, and TGF-β1 groups compared with the NG+MA group (Fig. 4A). Treatment with antioxidant NAC, LY-294002, SB-431542 or rapamycin significantly delayed wound closure (Fig. 4A). Similarly, treatment with antioxidant NAC, LY-294002, SB-431542 or rapamycin significantly reduced the migration of NRK-52E cells across Transwell chambers in HG conditions (Fig. 4B). These results suggest that inhibition of the ROS-mediated TGF-β1/PI3K/Akt/mTOR pathway results in a significant reduction in cell migration and invasion.

Table II. Blood glucose and renal function of diabetic rats.

Group	Fasting blood glucose (mmol/l)	Creatinine (μmol/l)	Blood urea nitrogen (mmol/l)	24 h urine protein (mg)
Normal	7.15±0.82	48.36±2.14	5.43±0.75	11.55±0.60
Diabetic model	29.74±2.51[a]	128.52±11.10[a]	18.70±4.72[a]	31.65±8.83[a]

[a]P<0.01 vs. the normal group.

Table III. Renal cortex and serum levels of GSH, T-SOD and MDA.

	GSH (mg/g protein)		T-SOD (U/mg protein)		MDA (μmol/g protein)	
Group	Renal cortex	Serum	Renal cortex	Serum	Renal cortex	Serum
Normal	1.98±0.53	2.63±0.41	78.92±16.31	142.29±11.17	0.89±0.36	1.24±0.27
Diabetic model	1.42±0.25[b]	0.69±0.33[b]	55.10±12.69[b]	69.32±18.54[b]	1.49±0.11[b]	2.08±0.63[a]

[a]P<0.05 and [b]P<0.01, vs. the normal group. GSH, glutathione; T-SOD, superoxide dismutase; MDA, malondialdehyde.

Blood glucose and renal function in the DM group. BUN, 24 h urine protein and Cr are important indicators of renal function. A rat model of diabetes was constructed using STZ. The results of the present study demonstrated that blood glucose, Cr, BUN and 24 h urine protein levels were significantly increased in the DM group compared with the N group, which suggests that DN was successfully induced (Table II).

Oxidative stress indicators are increased in rats with diabetes. GSH, T-SOD and MDA are important indicators of the oxidative stress index (31). In the present study, GSH and T-SOD expression were decreased in the renal cortex and serum of the DM group compared with the N group, while MDA levels were significantly increased (Table III).

Renal fibrosis is induced by PI3K/Akt/mTOR signalling in rats with diabetes. The relative expression of TGF-β1 was increased in the DM group compared with the N group (Fig. 5A). Furthermore, the phosphorylation of Akt (Ser473) and mTOR (Ser2448) were significantly increased in the kidneys of diabetic rats (Fig. 5B and C) compared with rats in the N group. Together, these results suggest that activation of the PI3K/Akt/mTOR pathway may induce EMT, leading to kidney fibrosis in diabetic rats.

Tubular epithelial cell EMT serves an important role in renal fibrosis. The levels of E-cadherin and α-SMA mRNA and protein in the renal cortex of rats were detected. The results demonstrated that diabetes caused a significant increase in α-SMA expression, while E-cadherin expression was significantly decreased compared with rats in the N group (Fig. 6A and B). To further explore kidney fibrosis in diabetes, the extent of mesangial matrix dilation was examined using periodic acid Schiff (PAS) staining (Fig. 6C). Positive PAS staining was significantly increased in rats from the DM group compared with those from the N group (Fig. 6C). Additionally, Masson staining revealed that kidney fibrosis was exacerbated in rats with diabetes compare with the N group (Fig. 6D).

Discussion

The excessive deposition of extracellular matrix in the glomeruli and renal tubules is a typical manifestation of DN, causing glomerulosclerosis and renal interstitial fibrosis (32). It has previously been reported that renal interstitial fibrosis serves an essential role in all types of progressive CKD (33). In the present study, interstitial changes to the kidney and the conventional parameters of 24-h urine protein, BUN and Cr were monitored. In order to observe the extent of kidney fibrosis, collagen and glycogen deposition were visualized using Masson and PAS staining. Collagen and glycogen accumulation was detected in the glomeruli, tubular basement membrane and kidney interstitial areas of rats with diabetes. These results suggest that kidney fibrosis is an important pathological feature of DN.

EMT is considered to be a major mechanism of renal fibrosis in DN (8). EMT of renal tubular epithelial cells is characterized by a loss of epithelial proteins, including E-cadherin, and increased expression of mesenchymal markers, including α-SMA (34). Changes in the expression of these proteins are generally accompanied by morphological changes from a cubic shape to a fibroblastoid appearance, as well as an increase in cell invasion and migration (4). A number of previous studies have reported that HG induces EMT via a number of factors and mechanisms (29,35,36), which is in agreement with the results of the present study. As well as the results of *in vitro* experiments, the present study demonstrated that E-cadherin expression was decreased and α-SMA expression was increased in rats with diabetes *in vivo*. Furthermore, wound-healing and Transwell chamber assays confirmed that HG induces migration and invasion in NRK-52E cells. These results demonstrate that HG conditions promote renal tubular EMT in diabetic nephropathy.

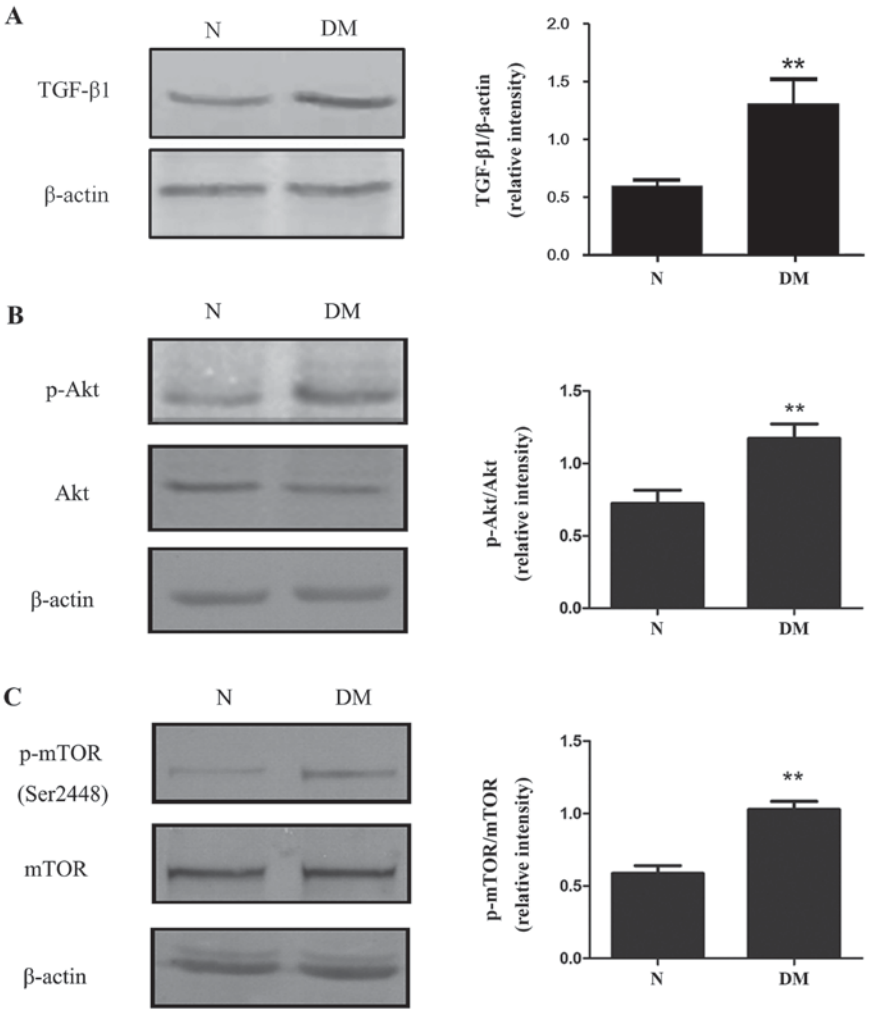

Figure 5. Expression of (A) TGF-β1, (B) Akt and (C) mTOR in the renal cortices of rats with diabetes. **P<0.01 vs. N. TGF, transforming growth factor; Akt, protein kinase B; mTOR, mammalian target of rapamycin; p, phosphorylated; N, normal control; DM, diabetic model.

ROS overproduction under hyperglycaemic conditions serves a core role in the pathogenesis of diabetic complications (11,12). ROS can cause DNA, protein and lipid injuries, as well as acting as signalling molecules in multiple pathways that cause cellular damage (9,37,38). The present study demonstrated that HG conditions increase ROS generation, decrease levels of T-SOD and GSH and increase MDA content, which suggests that HG aggravates oxidative stress in NRK-52E cells and rats with diabetes. However, treatment with antioxidant NAC effectively inhibits ROS generation in an HG environment. NAC also increased the expression of E-cadherin, reduced the expression of α-SMA, significantly delayed wound closure and prevented the migration of NRK-52E cells across the Transwell chamber. These results suggest that ROS serves a role in the development of EMT.

ROS is associated with EMT induced by TGF-β1, aldosterone, albumin or oxidized low-density lipoprotein, which is consistent with earlier studies (39). The upregulation of TGF-β1 *in vitro* and *in vivo* serves a significant role in the pathogenesis of DN (15,40) and it was demonstrated that TGF-β1 expression was increased under HG conditions. H_2O_2, which was used as an agent to simulate oxidative stress, also increased the expression of TGF-β1. However, the expression of TGF-β1 was significantly downregulated with NAC treatment under HG conditions. Thus, these results suggest that TGF-β1 upregulation in NRK-52E cells and diabetic rats is due, in part, to the excessive production of ROS under HG conditions.

It has been confirmed that the classic TGF-β1-Smad pathway is able to mediate the pathogenesis of fibrosis. Non-Smad-dependent pathways downstream of TGF-β1 have been reported to serve important roles in the occurrence and development of EMT, the P13K/Akt signaling pathway is particularly important (41). The results of the present study revealed that the expression of phosphorylated-Akt was increased in HG and diabetic conditions, while treatment with NAC, LY-294002 and SB-431542 groups decreased the phosphorylation of Akt *in vitro*. The results of the present study indicate that the TGF-β1/PI3K/Akt pathway may be positively activated by excessive production of ROS in diabetes.

mTOR is a serine/threonine kinase, which belongs to the family of phosphatidylinositol kinase-related kinase (PIKK) (23). A number of cell signals are mediated by mTOR, including nutrients, energy and growth factors, to regulate transcription, translation, autophagy and ribosome biogenesis (23-26). Previous animal and clinical studies have reported that mTOR serves a role in diabetic nephropathy and that the inhibition of mTORC1 with rapamycin

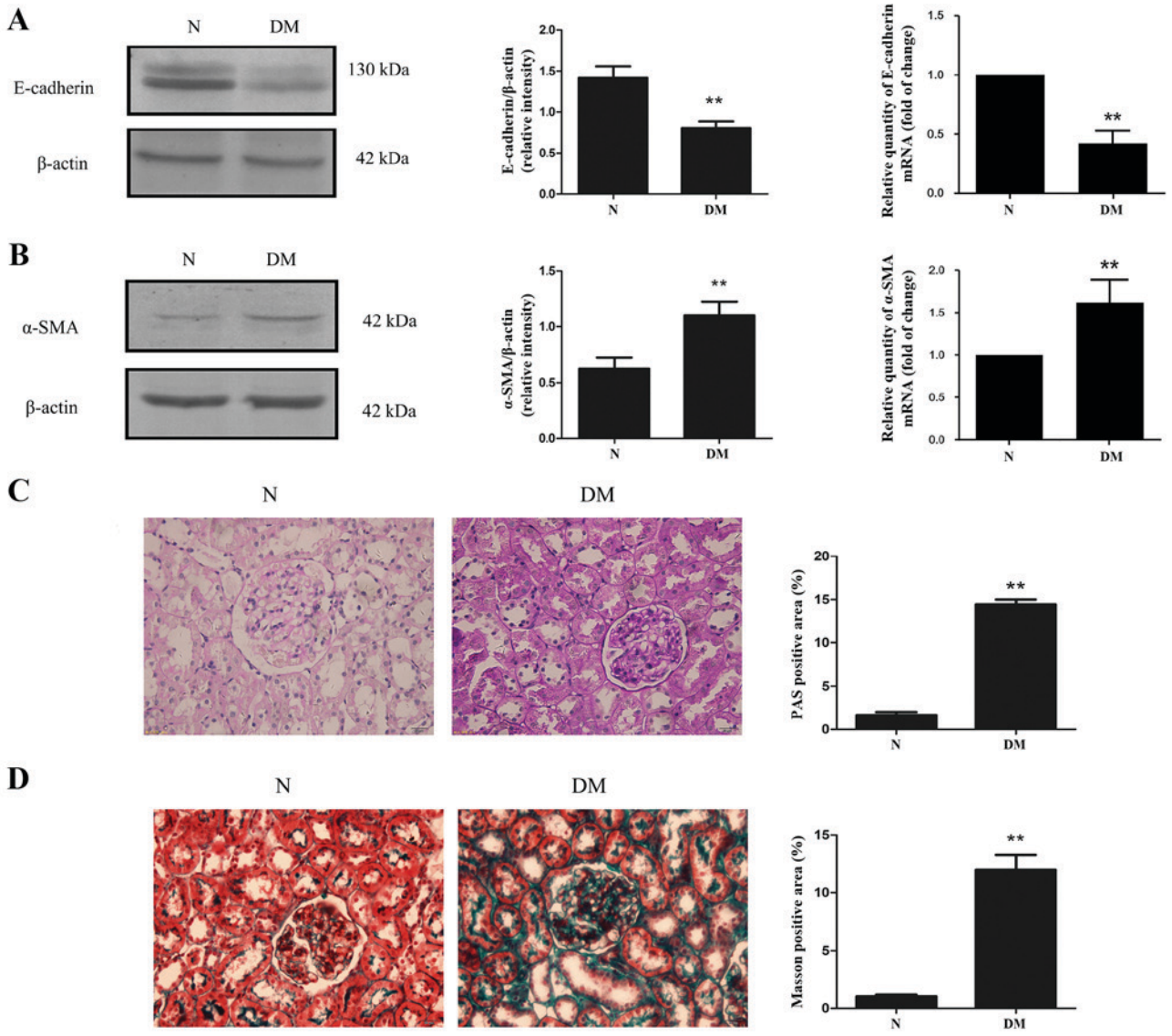

Figure 6. Expression of (A) E-cadherin and (B) α-SMA in the renal cortices of rats with diabetes. Accumulation of (C) glycogen and (D) collagens in the renal cortices of rats with diabetes. **P<0.01 vs. N. E-cadherin, epithelial cadherin; SMA, smooth muscle actin; normal control; DM, diabetic model.

attenuates morphological and functional disorders in diabetic kidneys (42,43). Furthermore, mTOR promotes interstitial fibrosis by enhancing the proliferation of fibroblasts and affects tubular EMT through profibrotic cytokines (26). In the present study, the effect of mTOR on HG-induced EMT was assessed and the possible mechanisms were explored. The results demonstrated that mTOR phosphorylation was significantly increased, wound closure was accelerated and migration was increased in the TGF-β1 and H_2O_2 groups compared with the NG+MA group. Similarly, the expression of p-mTOR was increased and kidney fibrosis was exacerbated in rats with diabetes. However, following treatment with NAC, SB-431542, LY-294002 or rapamycin, p-mTOR was decreased and cell migration and invasion were delayed, preventing the progression of EMT in NRK-52E cells. These results suggest that mTOR regulates EMT in HG conditions via the TGF-β1/PI3K/Akt signalling pathway. This is in agreement with a previous study, in which it was demonstrated that PI3K/Akt was activated during TGF-β1-induced EMT in cancer cells (44).

In summary, the present study demonstrates HG induces ROS generation, which activates the PI3K/Akt signalling pathway via TGF-β1 upregulation, leading to mTOR phosphorylation, EMT and accelerated renal fibrosis in DN.

Acknowledgements

The authors would like to thank Mrs Chen Sha (Nanjing University of Traditional Chinese Medicine, Nanjing, China) for the donation of the normal rat kidney tubular epithelial cell line (NRK-52E).

Funding

The present study was supported by the National Natural Science Foundation of China (grant nos. 81473257 and 81400741), the Qian Lan Project, the Natural Science Foundation of Jiangsu Province (grant no. BK20151155), the '333' Foundation of the Jiangsu Province (grant no. BRA2015329), the Key Natural Science Foundation of the Jiangsu Higher Education

Institutions of China (grant no. 15KJA310005), Jiangsu Overseas Research and Training Program for University Prominent Young and Middle-aged Teachers and Presidents and the Priority Academic Program Development of Jiangsu Higher Education Institutions (PAPD).

Availability of data and materials

All data generated or analysed during this study are included in this published article.

Authors' contributions

QL and XXY designed and supervised the study. WWW, MZZ, ZXM and XRQ performed the experiments and analyzed the data. MS analyzed the data.

Ethics approval and consent to participate

The present study was approved by the Animal Ethics Committee of Xuzhou Medical University (Xuzhou, China) and all experiments were performed in accordance with the Guidelines for Ethical Conduct in the Care and Use of Animals.

Consent for publication

Not applicable.

Competing interests

The authors declare that there are no competing interests.

References

1. Cooper ME: Pathogenesis, prevention, and treatment of diabetic nephropathy. Lancet 352: 213-219, 1998.
2. Kanwar YS, Sun L, Xie P, Liu FY and Chen S: A glimpse of various pathogenetic mechanisms of diabetic nephropathy. Annu Rev Pathol 6: 395-423, 2011.
3. Eddy AA: Molecular basis of renal fibrosis. Pediatr Nephrol 15: 290-301, 2000.
4. Zeisberg M and Neilson EG: Biomarkers for epithelial-mesenchymal transitions. J Clin Invest 119: 1429-1437, 2009.
5. Hu N, Duan J, Li H, Wang Y, Wang F, Chu J, Sun J, Liu M, Wang C, Lu C and Wen A: Hydroxysafflor yellow a ameliorates renal fibrosis by suppressing TGF-β1-induced epithelial-to-mesenchymal transition. PLoS One 11: e0153409, 2016.
6. Burns WC and Thomas MC: Angiotensin II and its role in tubular epithelial to mesenchymal transition associated with chronic kidney disease. Cells Tissues Organs 193: 74-84, 2011.
7. Yang YL, Ju HZ, Liu SF, Lee TC, Shih YW, Chuang LY, Guh JY, Yang YY, Liao TN, Hung TJ and Hung MY: BMP-2 suppresses renal interstitial fibrosis by regulating epithelial mesenchymal transition. J Cell Biochem 112: 2558-2565, 2011.
8. Liu Y: Epithelial to mesenchymal transition in renal fibrogenesis: Pathologic significance, molecular mechanism, and therapeutic intervention. J Am Soc Nephrol 15: 1-12, 2004.
9. Rösen P, Nawroth PP, King G, Möller W, Tritschler HJ and Packer L: The role of oxidative stress in the onset and progression of diabetes and its complications: A summary of a congress series sponsored by UNESCO-MCBN, the American diabetes association and the German diabetes society. Diabetes Metab Res Rev 17: 189-212, 2001.
10. Giacco F and Brownlee M: Oxidative stress and diabetic complications. Circ Res 107: 1058-1070, 2010.
11. Kashihara N, Haruna Y, Kondeti VK and Kanwar YS: Oxidative stress in diabetic nephropathy. Curr Med Chem 17: 4256-4269, 2010.
12. Brownlee M: The pathobiology of diabetic complications: A unifying mechanism. Diabetes 54: 1615-1625, 2005.
13. Smith KA, Zhou B, Avdulov S, Benyumov A, Peterson M, Liu Y, Okon A, Hergert P, Braziunas J, Wagner CR, *et al*: Transforming growth factor-β1 induced epithelial mesenchymal transition is blocked by a chemical antagonist of translation factor eIF4E. Sci Rep 5: 18233, 2015.
14. Shirakihara T, Horiguchi K, Miyazawa K, Ehata S, Shibata T, Morita I, Miyazono K and Saitoh M: TGF-β regulates isoform switching of FGF receptors and epithelial-mesenchymal transition. EMBO J 30: 783-795, 2011.
15. Hills CE and Squires PE: The role of TGF-β and epithelial-to mesenchymal transition in diabetic nephropathy. Cytokine Growth Factor Rev 22: 131-139, 2011.
16. Ji Y, Dou YN, Zhao QW, Zhang JZ, Yang Y, Wang T, Xia YF, Dai Y and Wei ZF: Paeoniflorin suppresses TGF-β mediated epithelial-mesenchymal transition in pulmonary fibrosis through a Smad-dependent pathway. Acta Pharmacol Sin 37: 794-804, 2016.
17. Kattla JJ, Carew RW, Heljic M, Godson C and Brazil DP: Protein kinase B/Akt activity is involved in renal TGF-beta1-driven epithelial-mesenchymal transition in vitro and in vivo. Am J Physiol Renal Physiol 295: F215-F225, 2008.
18. Risso G, Blaustein M, Pozzi B, Mammi P and Srebrow A: Akt/PKB: One kinase, many modifications. Biochem J 468: 203-214, 2015.
19. Lu Q, Zhai Y, Cheng Q, Liu Y, Gao X, Zhang T, Wei Y, Zhang F and Yin X: The Akt-FoxO3a-manganese superoxide dismutase pathway is involved in the regulation of oxidative stress in diabetic nephropathy. Exp Physiol 98: 934-945, 2013.
20. Lu Q, Zuo WZ, Ji XJ, Zhou YX, Liu YQ, Yao XQ, Zhou XY, Liu YW, Zhang F and Yin XX: Ethanolic *Ginkgo biloba* leaf extract prevents renal fibrosis through Akt/mTOR signaling in diabetic nephropathy. Phytomedicine 22: 1071-1078, 2015.
21. Bai X and Jiang Y: Key factors in mTOR regulation. Cell Mol Life Sci 67: 239-253, 2010.
22. Ma XM and Blenis J: Molecular mechanisms of mTOR-mediated translational control. Nat Rev Mol Cell Biol 10: 307-318, 2009.
23. Inoki K: Role of TSC-mTOR pathway in diabetic nephropathy. Diabetes Res Clin Pract 82 (Suppl 1): S59-S62, 2008.
24. Lin CJ, Chen TL, Tseng YY, Wu GJ, Hsieh MH, Lin YW and Chen RW: Honokiol induces autophagic cell death in malignant glioma through reactive oxygen species-mediated regulation of the p53/PI3K/Akt/mTOR signaling pathway. Toxicol Appl Pharmacol 304: 59-69, 2016.
25. Yalcin S, Marinkovic D, Mungamuri SK, Zhang X, Tong W, Sellers R and Ghaffari S: ROS-mediated amplification of AKT/mTOR signalling pathway leads to myeloproliferative syndrome in Foxo3(-/-) mice. EMBO J 29: 4118-4131, 2010.
26. Fantus D, Rogers NM, Grahammer F, Huber TB and Thomson AW: Roles of mTOR complexes in the kidney: Implications for renal disease and transplantation. Nat Rev Nephrol 12: 587-609, 2016.
27. Lieberthal W and Levine JS: The role of the mammalian target of rapamycin (mTOR) in renal disease. J Am Soc Nephrol 20: 2493-2502, 2009.
28. Lamouille S and Derynck R: Emergence of the phosphoinositide 3-kinase-Akt-mammalian target of rapamycin axis in transforming growth factor-β-induced epithelial-mesenchymal transition. Cells Tissues Organs 193: 8-22, 2011.
29. Lu Q, Ji XJ, Zhou YX, Yao XQ, Liu YQ, Zhang F and Yin XX: Quercetin inhibits the mTORC1/p70S6K signaling-mediated renal tubular epithelial-mesenchymal transition and renal fibrosis in diabetic nephropathy. Pharmacol Res 99: 237-247, 2015.
30. Schmittgen TD and Livak KJ: Analyzing real-time PCR data by the comparative C(T) method. Nat Protoc 3: 1101-1108, 2008.
31. Ha H, Yang Y and Lee HB: Mechanisms of reactive oxygen species generation in LLC-PKI cells cultured under high glucose. J Am Sec Nephrol 13: 531, 2002.
32. Brosius FC, Khoury CC, Buller CL and Chen S: Abnormalities in signaling pathways in diabetic nephropathy. Expert Rev Endocrinol Metab 5: 51-64, 2010.
33. Simonson MS: Phenotypic transitions and fibrosis in diabetic nephropathy. Kidney Int 71: 846-854, 2007.
34. Liu Y: New insights into epithelial-mesenchymal transition in kidney fibrosis. J Am Soc Nephrol 21: 212-222, 2010.
35. Lv ZM, Wang Q, Wan Q, Lin JG, Hu MS, Liu YX and Wang R: The role of the p38 MAPK signaling pathway in high glucose-induced epithelial-mesenchymal transition of cultured human renal tubular epithelial cells. PLoS One 6: e22806, 2011.

36. Liu R, Wang Y, Xiao Y, Shi M, Zhang G and Guo B: SnoN as a key regulator of the high glucose-induced epithelial-mesenchymal transition in cells of the proximal tubule. Kidney Blood Press Res 35: 517-528, 2012.
37. Brownlee M: Biochemistry and molecular cell biology of diabetic complications. Nature 414: 813-820, 2001.
38. Coughlan MT, Mibus AL and Forbes JM: Oxidative stress and advanced glycation in diabetic nephropathy. Annals of the New York Academy of Sciences 1126: 190-193, 2008.
39. Wang R, Ding G, Liang W, Chen C and Yang H: Role of LOX-1 and ROS in oxidized low-density lipoprotein induced epithelial-mesenchymal transition of NRK52E. Lipids Health Dis 9: 120, 2010.
40. Tang F, Hao Y, Zhang X and Qin J: Effect of echinacoside on kidney fibrosis by inhibition of TGF-β1/Smads signaling pathway in the db/db mice model of diabetic nephropathy. Drug Des Devel Ther 11: 2813-2826, 2017.
41. Suwanabol PA, Seedial SM, Zhang F, Shi X, Si Y, Liu B and Kent KC: TGF-β and Smad3 modulate PI3K/Akt signaling pathway in vascular smooth muscle cells. Am J Physiol Heart Circ Physiol 302: H2211-H2219, 2012.
42. Chen JK, Chen J, Neilson EG and Harris RC: Role of mammalian target of rapamycin signaling in compensatory renal hypertrophy. J Am Soc Nephrol 16: 1384-1391, 2005.
43. Lee CH, Inoki K and Guan KL: mTOR pathway as a target in tissue hypertrophy. Annu Rev Pharmacol Toxicol 47: 443-467, 2007.
44. Yeh YH, Wang SW, Yeh YC, Hsiao HF and Li TK: Rhapontigenin inhibits TGF-β-mediated epithelial-mesenchymal transition via the PI3K/AKT/mTOR pathway and is not associated with HIF-1α degradation. Oncol Rep 35: 2887-2895, 2016.